Physica B 405 (2010) 2061–2064

Contents lists available at ScienceDirect

Physica B

journal homepage: www.elsevier.com/locate/physb

The structure optimization design of the organic solar cells using the FDTD method

Jian Wang [a], Cheng-Wei Wang [a,*], Yan Li [a], Feng Zhou [b], Wei-Min Liu [b]

[a] College of Physics and Electronic Engineering, Northwest Normal University, Lanzhou 730070, PR China
[b] State Key Laboratory of Solid Lubrication, Lanzhou Institute of Chemical Physics, Chinese Academy of Sciences, Lanzhou 730000, PR China

ARTICLE INFO

Article history:
Received 19 November 2009
Received in revised form
16 January 2010
Accepted 18 January 2010

Keywords:
Organic solar cells
The finite-different time-domain method (FDTD)
The optical electrical field energy
Optimization design

ABSTRACT

The finite-different time-domain method (FDTD) was used to optimize structure of organic solar cells based on the heterojunction of the substituted polythiophene polymer (PEOPT) and the C_{60} molecule. The absorption of the device in visible light range was determined, and the maximized average absorption is about 88% at the wavelength of 469 nm. The effects of the glass substrate thickness on the absorption and the distribution of the optical energy inside the device were investigated. Based on the important roles of the optical energy at PEOPT/C_{60} interface in the photocurrent efficiency, the device structure was optimized for the maximized photocurrent efficiency. The optimal C_{60} thickness 29 nm was obtained for the wavelength of 469 nm. Meantime, when the PEOPT thickness is the range of 80–130 nm, there are few effects on optical energy at PEOPT/C_{60} interface.

1. Introduction

Organic solar cells have recently been proposed as a key for energy supply because they cover a large area, have a low cost, and produce flexible solar cells [1–3]. By incorporating multilayers and bulk heterojunctions, the energy conversion efficiency of organic solar cells was gradually increased to around 5% [4–5]. The high conversion efficiency is the result of efficient absorption of light and charge generation inside the devices. Presently there are some controversies in mechanism for organic solar cells, but the mechanism for generation of photocurrent in organic thin film solar cells is believed to be due to the creation of bound electro-hole pairs, excitons, by absorption of light in the active layers of the devices [6–9]. Charge generation occurs as a result of dissociation of the excitons by interaction of the excitons with the interfaces, impurities of defects, or in high electrical fields. So the incorporation of dissociation sites is the reason for higher efficiency of devices made of blends and bilayer. In the case of thin film solar cells, a number of layers are stacked on top of each other in a multilayer configuration. Reflections at interfaces affect the distribution of the optical electrical field inside the thin film solar cells. The generation of excitons is directly dependent on the distribution of the optical electrical field energy inside the device, which consequently will influence the photocurrent characteristics of the device. For the reason, the distribution of the optical electrical field energy inside the device is an important to optimize the structure of organic solar cell for excellent performance.

Many works have been done to calculate the distribution of the optical electrical field energy inside the thin film solar cells, to calculate the transmission and reflection of organic solar cells [10–12]. The finite-different time-domain method (FDTD) has been widely used to simulate the transient solution of electromagnetic wave propagation in the dispersive medium, its major advantage is its ability to provide a full spectrum in a single simulation by propagating a short pulse in the time-domain, and it is comparatively easy, exact and effective. So in the paper, the FDTD method was used to calculate the distribution of the optical electrical field energy inside the organic thin film solar cells formed by a heterojunction of the substituted polythiophene polymer (PEOPT) and the C_{60} molecule, sandwiched between anode of indium-tin oxide (ITO)/poly (3,4-ethylenedioxythiophene) (PEDOT) and cathode of Al. Because the efficiency of the organic solar cell is dependent on the distribution of the internal optical electric field, the geometrical structure of the solar cells is important for enhancing its efficiency. Based on the calculated distribution of the internal optical electric field inside the device, the thickness of C_{60} layer and PEOPT layer was optimized to enhance the efficiency of the organic solar cell.

2. Materials and methods

The FDTD method treats the Maxwell equations as a set of finite difference equations in both time and space. In an isotropic

* Corresponding author. Tel./fax: +86 9317971503.
E-mail address: cwwang@nwnu.edu.cn (C.-W. Wang).

0921-4526/$ - see front matter © 2010 Elsevier B.V. All rights reserved.
doi:10.1016/j.physb.2010.01.102

medium, Maxwell's equations and the related equations are given as follows:

$$\frac{\partial \vec{D}}{\partial t} = \nabla \times \vec{H}, \tag{1}$$

$$\frac{\partial \vec{H}}{\partial t} = -\frac{1}{\mu_0} \nabla \times \vec{E}, \tag{2}$$

$$\vec{D}(\omega) = \varepsilon_0 \cdot \varepsilon_r^*(\omega) \cdot \vec{E}(\omega), \tag{3}$$

where $\vec{D}$ is the electric flux density, $\vec{E}$ and $\vec{H}$ are the electric field and magnetic field intensities respectively. The Eqs. (1) and (2) can be normalized by using the following relations:

$$\tilde{\vec{E}} = \sqrt{\frac{\varepsilon_0}{\mu_0}} \cdot \vec{E}, \tag{4}$$

$$\tilde{\vec{D}} = \sqrt{\frac{1}{\varepsilon_0 \cdot \mu_0}} \cdot \vec{D}, \tag{5}$$

which lead to

$$\frac{\partial \tilde{\vec{D}}}{\partial t} = \frac{1}{\sqrt{\varepsilon_0 \mu_0}} \nabla \times \vec{H}, \tag{6}$$

$$\frac{\partial \vec{H}}{\partial t} = -\frac{1}{\sqrt{\varepsilon_0 \mu_0}} \nabla \times \tilde{\vec{E}}, \tag{7}$$

$$\tilde{\vec{D}}(\omega) = \varepsilon_r^*(\omega) \cdot \tilde{\vec{E}}(\omega), \tag{8}$$

where $\tilde{\vec{D}}$, $\tilde{\vec{E}}$, $\vec{H}$ are vectors in three dimensions, so in general, Eqs. (6) and (7) represent three equations each. For one-dimensional case, only $\tilde{D}_x$, $\tilde{E}_x$ and H_y are used, so the Eqs. (6) and (7) can be written as follows:

$$\frac{\partial \tilde{D}_x}{\partial t} = -\frac{\partial H_y}{\partial z}, \tag{9}$$

$$\frac{\partial H_y}{\partial t} = -\frac{1}{\mu_0} \frac{\partial \tilde{E}_x}{\partial z}. \tag{10}$$

In Eq. (8), the parameter ε_r^* is relative complex dielectric constant. In general, parameter ε_r^* has the following form in frequency domain:

$$\varepsilon_r^*(\omega) = \varepsilon_r(\omega) + j\frac{\sigma(\omega)}{\omega \varepsilon_0} \tag{11}$$

where j is $\sqrt{-1}$ and ω is angular frequency. Meanwhile, the relative complex dielectric constant ε_r^* can also be written as $\varepsilon_r^* = \varepsilon_r' + j\varepsilon_r''$, the real part ε_r' and the imaginary part ε_r'' can be given by the following the relations:

$$\varepsilon_r' = n^2(\omega) - k^2(\omega) \tag{12}$$

$$\varepsilon_r''(\omega) = 2n(\omega)k(\omega) \tag{13}$$

where $n(\omega)$ and $k(\omega)$ are the refractive index and the extinction coefficient whose relation with the relatively dielectric constant $\varepsilon_r(\omega)$ and conductivity $\sigma(\omega)$ in Eq. (11) can be obtained:

$$\varepsilon_r(\omega) = n^2(\omega) - k^2(\omega) \tag{14}$$

$$\sigma(\omega) = 2n(\omega)k(\omega)\omega\varepsilon_0 \tag{15}$$

Certainly, the dispersion relation of refractive index $n(\omega)$ and extinction coefficient $k(\omega)$ can be measured.

However, for the metal, such as Al, Au and Ag, the relative complex dielectric constant ε_r^* should be satisfied with the Drude model:

$$\varepsilon_r^*(\omega) = 1 + \frac{\omega_p^2}{\omega(j\upsilon_c - \omega)} \tag{16}$$

where ω_p is the plasma frequency, υ_c is the electron collision frequency.

In the simulation process, the FDTD cell size Δz should be satisfied with the relation $\Delta z \le \lambda/10$, where λ is the incident wavelength. Once the Δz is chosen, then the time step Δt is determined by $\Delta t = \Delta z/2 \cdot c_0$, where c_0 is the speed of light in free space.

3. Results and discussion

The organic heterojunction solar cells studied in the work had the thin film structure as shown in Fig. 1. Some works have proved that the PEDOT/PEOPT interface is more beneficial to the collection of holes compared to the ITO/PEOPT interface [10]. So in order to get improved current–voltage characteristics of the device, the polymer PEDOT was coated onto the ITO/glass substrate used as hole collecting electrode. The donor–acceptor heterojunction is built up by the polymer PEOPT and the C_{60}. The Al was used as electron collecting electrode.

The total absorption A of the solar cells is an important parameter to evaluate their performance. It represents the upper limit for the fraction of incident photons at the device that can contribute to the photocurrent, and also be the upper limit for the photon to current collection efficiency of this particular device. In the organic solar cells, the Al layer is much thicker than the penetration depth of light in the visible light range, and its transmission is zero. So the total absorption A is described as $A = 1 - R$, where R is the reflectance of the solar cells. In the actual application of the investigated glass/ITO (120 nm)/PEDOT (110 nm)/PEOPT (40 nm)/C_{60} (30 nm)/Al device, the glass substrate is transparent, and its thickness is generally 2 mm which is much larger than the wavelength of the visible light. So there is not the interference fringes resulted from the glass substrate in the absorption spectra. However, in FDTD simulation process, the large glass substrate thickness will greatly increase the calculation amounts and time. Thus, in order to decrease the calculation amounts and time, the thicknesses of the glass substrate are made as 5, 10, 15, 20 and 25 μm in the calculation of the total absorption A of the investigated organic thin film solar cells, as shown in Fig. 2. Certainly, in the FDTD simulation process, the optical parameters $n(\omega)$ and $k(\omega)$ of each layer in the organic solar cell are necessary, and could be obtained from references. The $n(\omega)$ and $k(\omega)$ of the C_{60} and PEOPT films were obtained from Ref. [10], the $n(\omega)$ and $k(\omega)$ of PEDOT films were obtained

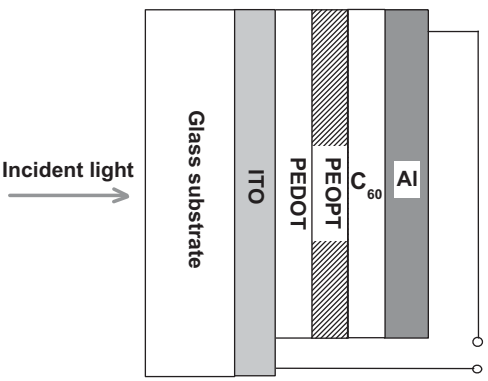

Fig. 1. The schematic presentation of the organic thin film solar cell structure: glass/ITO/PEDOT/PEOPT/C_{60}/Al.

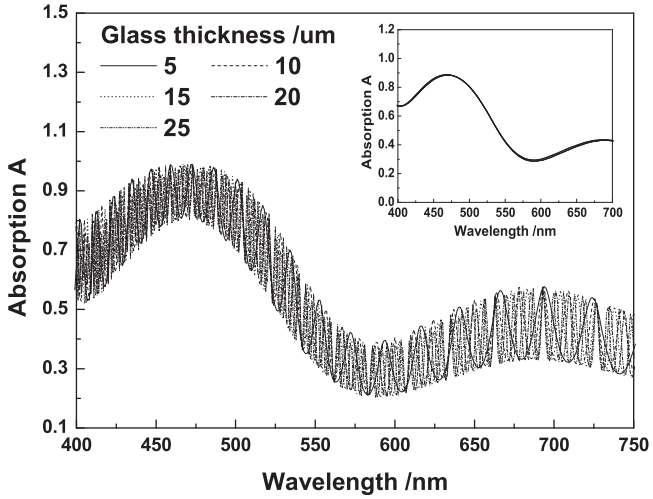

Fig. 2. The calculated absorption of the glass/ITO (120 nm)/PEDOT (110 nm)/PEOPT (40 nm)/C_{60} (30 nm)/Al with the different glass substrate thickness using FDTD method. The inset is the corresponding average absorption.

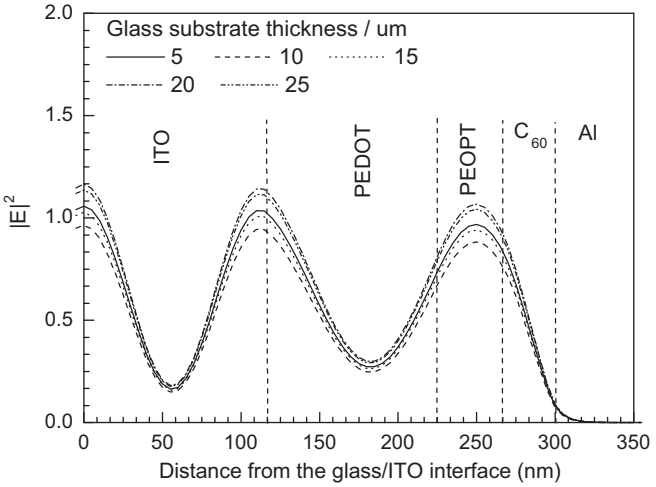

Fig. 3. The calculated distribution of the optical electrical field energy inside the glass/ITO (120 nm)/PEDOT (110 nm)/PEOPT (40 nm)/C_{60} (30 nm)/Al device with the glass substrate thickness of 5, 10, 15, 20, and 25 μm for the wavelength of 469 nm by using the FDTD method.

from Ref. [13], the optical constants of ITO films were obtained from Ref. [14] and the optical constants of metal Al and glass substrate referred to Ref. [15]. Obviously, the thicknesses of glass substrate are close to the wavelength of the visible light, and the absorption spectra of these solar cells were enclosed the interference fringes. But all average absorption spectra of the devices are same, shown in the inset of Fig. 2. That is, the transparent glass substrate thickness has no effect on the average absorption of the thin film solar cells, and the average absorption spectra is also same with that of the solar cell with the glass substrate thickness of 2 mm. Consequently, the maximum absorption of the investigated organic thin film solar cells with the glass substrate thickness of 2 mm is about 88% of the incident photons at the wavelength 469 nm. If all these absorbed photons would contribute to the photocurrent, then the photon to current collection efficiency would attain 88%. Of course, this is impossible. But the value of the maximum absorption is still very important to the performance evaluation of the solar cells.

It is well known that the generation of the excitons at the particular position inside the thin film solar cells is proportional to the product of the modulus squared of the electric field, the refractive index, and the absorption coefficient. Thus, the generation of the excitons can be obtained by the calculation of the distribution of the internal optical electric field. The distribution of the optical electric field inside the glass/ITO (120 nm)/PEDOT (110 nm)/PEOPT (40 nm)/C_{60} (30 nm)/Al device with the glass substrate thickness of 5, 10, 15, 20 and 25 μm was calculated for the wavelength of 469 nm, shown in Fig. 3. It is clear that only the peak values of the distribution of the optical electric field inside the solar cells varies with the increase of the glass substrate thickness, which is mainly due to the optical interference resulted from the small glass substrate thickness. Thus, the glass substrate thickness has few effects on the distribution of the optical electric field inside the solar cells when the thickness of glass substrate is much greater than the light wavelength. However, the thickness of C_{60} and PEOPT layers has strong effect on the distribution of the internal optical electric field, as shown in Figs. 4 and 5. So, the thickness of the PEOPT layer and the C_{60} layer can modulate the performance of the organic solar cell.

The C_{60}/Al interface is the most dominant boundary condition inside the solar cell, and to a large extent, it is also determining the distribution of excitons inside the device. However, in the

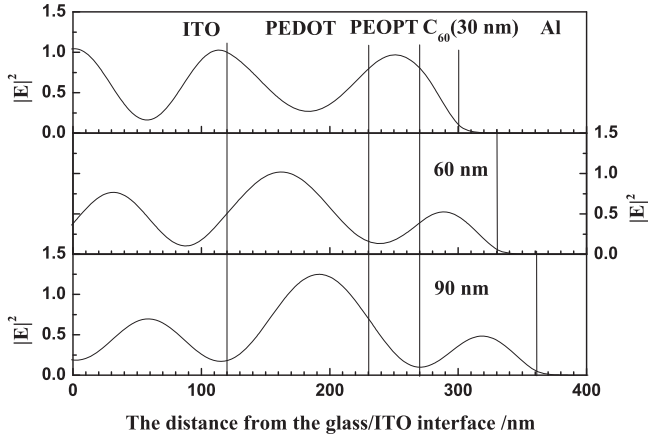

Fig. 4. The calculated distribution of the optical electrical field energy inside the glass/ITO (120 nm)/PEDOT (110 nm)/PEOPT (40 nm)/C_{60}/Al device with the C_{60} layer thickness of 30, 60 and 90 nm for the wavelength of 469 nm by using the FDTD method.

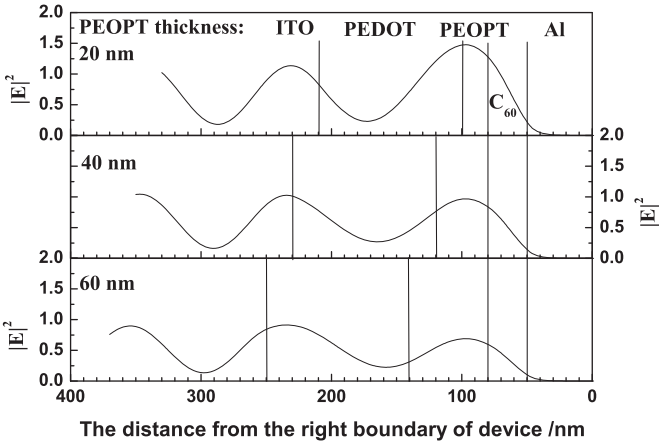

Fig. 5. The calculated distribution of the optical electrical field energy inside the glass/ITO (120 nm)/PEDOT (110 nm)/PEOPT/C_{60} (30 nm)/Al device with the PEOPT layer thickness of 20, 40 and 60 nm for the wavelength of 469 nm by using the FDTD method.

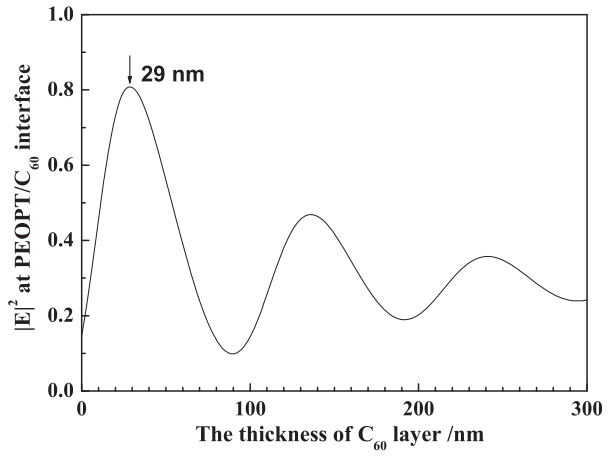

Fig. 6. The calculated optical electrical field energy at the PEOPT/C_{60} interface inside the glass/ITO (120 nm)/PEDOT (110 nm)/PEOPT (40 nm)/C_{60}/Al device versus the C_{60} layer thickness for the wavelength of 469 nm.

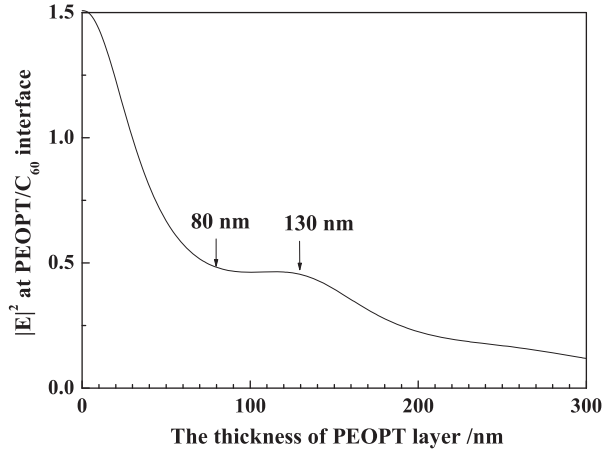

Fig. 7. The calculated optical electrical field energy at the PEOPT/C_{60} interface inside the glass/ITO (120 nm)/PEDOT (110 nm)/PEOPT/C_{60} (29 nm)/Al device versus the PEOPT layer thickness for the wavelength of 469 nm.

device, only these excitons that reach the dissociation site would contribute to the photocurrent due to the limited diffusion range of the excitons. The PEOPT/C_{60} interface is the active interface inside the device, and acts as a dissociation site for excitons. Therefore, in order to maximize the number of excitons at the PEOPT/C_{60} interface, the modulus squared of optical electric field at this interface will become important. Thus, it is viable to optimize the structure of the thin film solar cell for the maximized optical electric field energy at the PEOPT/C_{60} interface for the proper wavelength. The normalized modulus square of the optical electric field at PEOPT/C_{60} interface inside the glass/ITO (120 nm)/PEDOT (110 nm)/PEOPT (40 nm)/C_{60}/Al device with different thickness of the C_{60} layer for the wavelength of 469 nm was calculated using the above mentioned FDTD method, as shown in Fig. 6. It is clear that the thickness of the C_{60} layer has strong influence on the optical electric field energy at the PEOPT/C_{60} interface, and the 29 nm is the optimal thickness of C_{60} layer to maximize the photocurrent efficiency for the wavelength of 469 nm. Therefore, the thickness of C_{60} layer was made as 29 nm, a similar result about the normalized modulus square of the optical electric field at PEOPT/C_{60} interface versus the active layer PEOPT thickness was calculated, as shown in Fig. 7. On the whole, the normalized modulus square of the optical electric field at PEOPT/C_{60} interface decreases with the increasing of the PEOPT layer thickness. But it keeps a constant in the range from 80 to 130 nm of the PEOPT layer thickness. It is worthy that the optimal thickness 29 nm of C_{60} layer calculated by the FDTD method to maximize the photocurrent efficiency of the device agrees well with the reported experimental results in Ref. [10]. So the relative simple FDTD method is very effective to optimize the structure of the organic thin film solar cells for the excellent performance.

4. Summary

In summary, a simple and effective FDTD method was introduced to optimize the structure of organic thin film solar cells. The total absorption of the glass/ITO/PEDOT/PEOPT/C_{60}/Al device was calculated, and the maximum absorption is about 88% at the wavelength 469 nm. Due to the importance of the normalized modulus square of the optical electric field at PEOPT/C_{60} interface inside the device, the distribution of the modulus squared of the electric field inside the device was calculated. The device structure was optimized for the maximized photocurrent efficiency. The PEOPT thickness has few effects on optical electric field energy at PEOPT/C_{60} interface when it is in the range of 80–130 nm. The optimal thickness of the C_{60} layer for the wavelength 469 nm is 29 nm and agrees well with the experimental results reported in other works. Thus, the FDTD method is a very effective method to study the organic solar cells. Furthermore, the thickness of the transparent glass substrate has little effects on the average absorption of the device and the distribution of the optical electric energy inside the thin film solar cells.

Acknowledgments

The Authors are grateful to the support of the National Natural Science Foundation of China (Grant no. 10774121, 10974155), the Natural Science Foundation of Gansu Province of China (Grant no. 0803RJZA102), the Foundation of Northwest Normal University (Grant no. NWNU-KJCXGC-03-22), and the Foundation of Education Bureau of Gansu Province of China (Grant no. 0801-09).

References

[1] S. Günes, H. Neugebauer, N.S. Sariciftci, Chem. Rev. 107 (2007) 1324.
[2] A. Holzhey, C. Uhrich, E. Brier, E. Reinhold, P. Bäuerle, K. Leo, M. Hoffmann, J. Appl. Phys. 104 (2008) 064510.
[3] C. Falkenberg, C. Uhrich, S. Olthof, B. Maennig, M.K. Riede, K. Leo, J. Appl. Phys. 104 (2008) 034506.
[4] J. Peet, J.Y. Kim, N.E. Coates, W.L. Ma, D. Moses, A.J. Heeger, G.C. Bazan, Nat. Mater. 6 (2007) 497.
[5] K. Shankar, G.K. Mor, M. Paulose, O.K. Varghese, C.A. Grimes, J. Non-Cryst. Solids 354 (2008) 2767.
[6] D.W. Sievers, V. Shrotriya, Y. Yang, J. Appl. Phys. 100 (2006) 114509.
[7] Y. Terao, H. Sasabe, C. Adachi, Appl. Phys. Lett. 90 (2007) 103515.
[8] L.J.A. Koster, E.C.P. Smits, V.D. Mihailetchi, P.W.M. Blom, Phys. Rev. B 72 (2005) 085205.
[9] L.H. Slooff, S.C. Veenstra, J.M. Kroon, D.J.D. Moet, J. Sweelssen, M.M. Koetse, Appl. Phys. Lett. 90 (2007) 143506.
[10] L.A.A. Pettersson, L.S. Roman, O. Inganäs, J. Appl. Phys. 86 (1999) 487.
[11] B.V. Andersson, D.M. Huang, A.J. Moulé, O. Inganäs, Appl. Phys. Lett. 94 (2009) 043302.
[12] J. Meiss, N. Allinger, M.K. Riede, K. Leo, Appl. Phys. Lett. 93 (2008) 103311.
[13] D.X. Zhu, W.D. Shen, H. Ye, X. Liu, H.Y. Zhen, J. Phys. D: Appl. Phys. 41 (2008) 235104.
[14] F.C. Lai, L.M. Lin, R.Q. Gai, Y.Z. Lin, Z.G. Huang, Thin Solid Films 515 (2007) 7387.
[15] E.D. Palik, Handbook of Optical Constants of Solids, Academic Press, INC, London, 1985.